Ingeniería y Competitividad
Vol 27 (2) 2025 doi: 10.25100/iyc.v27i2.14759

Vol 27 (2)

ISSN
0123-3033
e- 2027-8284

Original Article

False positives and negatives in human-robot collision prevention: a virtual reality evaluation

Falsos positivos y negativos en la prevención de colisiones humano-robot: evaluación en realidad virtual

Juan J. Piamba[1] Carlos F. Rengifo[1] Diego E. Guzmán[2]

[1] Universidad del Cauca, Popayán, Colombia.
[2] Universidad Nacional Abierta y a Distancia (UNAD), Bogotá, Colombia.

Abstract

Introduction: in human-robot collaboration (HRC), accurately detecting the proximity of the operator is essential to ensure safety without compromising productivity. However, conventional distance sensors face a trade-off between false positives (FP), which may cause unnecessary robot stops, and false negatives (FN), which can lead to dangerous collisions.
Objectives: this study aims to analyze the balance between FP and FN in proximity detection within HRC environments using a virtual reality (VR) framework. The goal is to identify optimal sensor configurations that minimize FN without excessively increasing FP.
Materials and Methods: a VR-based simulation environment was developed to evaluate different parameters: detection range, sensor beam angle, and sensor placement on the robot. An ANOVA model and post-hoc tests were applied to assess the statistical impact of each variable. Additionally, a second experiment was conducted involving a human participant to observe sensor behavior under realistic human intervention conditions.
Results: the analysis identified sensor configurations that significantly reduce FN without notably increasing FP. Sensor beam angle and spatial coverage were found to be key factors. Tests involving human presence revealed additional challenges due to human movement variability and the need to fine-tune system sensitivity.
Conclusions: the findings provide key technical criteria for sensor selection and configuration in collaborative applications. Strategies to mitigate FP are proposed, including the integration of advanced technologies such as computer vision and millimeter-wave radar sensors. This work contributes to the design of safer and more efficient systems for human-robot interaction in industrial settings.

Keywords: Human-Robot Collaboration, Virtual Reality, Collision Detection, Collaborative Manufacturing.

Resumen

Introducción: en la colaboración humano-robot (HRC), detectar con precisión la proximidad del operador es esencial para garantizar la seguridad sin comprometer la productividad. Sin embargo, los sensores de distancia convencionales enfrentan una disyuntiva entre falsos positivos (FP), que pueden provocar paradas innecesarias del robot, y falsos negativos (FN), que pueden derivar en colisiones peligrosas.
Objetivos: este estudio tiene como objetivo analizar el equilibrio entre FP y FN en la detección de proximidad en entornos HRC, utilizando un entorno de realidad virtual (VR). Se busca identificar configuraciones óptimas de sensores que minimicen los FN sin incrementar excesivamente los FP.
Materiales y Métodos: se diseñó un entorno de simulación en VR en el que se evaluaron distintos parámetros: distancia de detección, ángulo de apertura del haz del sensor y disposición espacial de los sensores en el robot. Se aplicó un modelo ANOVA y pruebas post-hoc para determinar el impacto estadístico de cada variable. Adicionalmente, se realizó una segunda prueba con la participación de un usuario humano, a fin de observar el comportamiento de los sensores en presencia realista de intervención humana.
Resultados: los análisis identificaron configuraciones de sensores que reducen significativamente los FN sin aumentar de forma considerable los FP. La disposición angular y la cobertura espacial de los sensores resultaron ser factores determinantes. Las pruebas con intervención humana revelaron desafíos adicionales relacionados con la variabilidad del movimiento humano y la necesidad de ajustar la sensibilidad del sistema.
Conclusiones: los resultados ofrecen criterios técnicos clave para la selección y configuración de sensores en aplicaciones colaborativas. Se proponen estrategias para mitigar FP, incluyendo la integración de tecnologías como visión artificial y sensores de radar de onda milimétrica. Este trabajo contribuye al diseño de sistemas más seguros y eficientes en la interacción humano-robot en entornos industriales.

Palabras clave: Colaboración Humano-Robot, Realidad Virtual, Detección de Colisiones, Manufactura Colaborativa.

How to cite?

Piamba JJ, Rengifo CF, Guzmán DE. False positives and negatives in human-robot collision prevention: a virtual reality evaluation. Ingeniería y Competitividad, 2025, 27(2)e-20714759

https://doi.org/10.25100/iyc.v27i2.14759

Received: 20/02/25
Reviewed: 25/03/25
Accepted: 21/04/25
Online: 28/05/25

Correspondence

juanpiamba@unicauca.edu.co

Contribution to the literature

Why was it conducted?
This study was conducted to address the safety and efficiency challenges in collaborative manufacturing environments by analyzing the trade-off between false positives (FP) and false negatives (FN) in human-robot collision avoidance. Physical experimentation with real robots for sensor configuration is time-consuming, costly, and poses safety risks. Therefore, a VR-based simulator was developed to replicate the UR3 collaborative robot environment and evaluate five key parameters: sensor layout, detection distance, angle detection, sampling frequency, and noise simulation. The objective was to understand how these factors influence FP and FN rates, providing a cost-effective, safe, and efficient tool for optimizing sensor configurations in human-robot interaction (HRI) contexts.

What were the most relevant results? What do they contribute?
The results showed that detection distance, angle detection, and sensor layout significantly impact the trade-off between false positives and false negatives. Specifically, the End-joint sensor layout minimized false negatives, enhancing safety, while the Lateral layout minimized false positives, improving operational efficiency. The findings highlight that optimizing sensor configurations requires balancing detection parameters to ensure safety without excessively compromising productivity. This study contributes by providing a virtual reality tool for pre-evaluating and optimizing distance sensor configurations, supporting safer and more efficient deployment of collaborative robots in industrial environments.

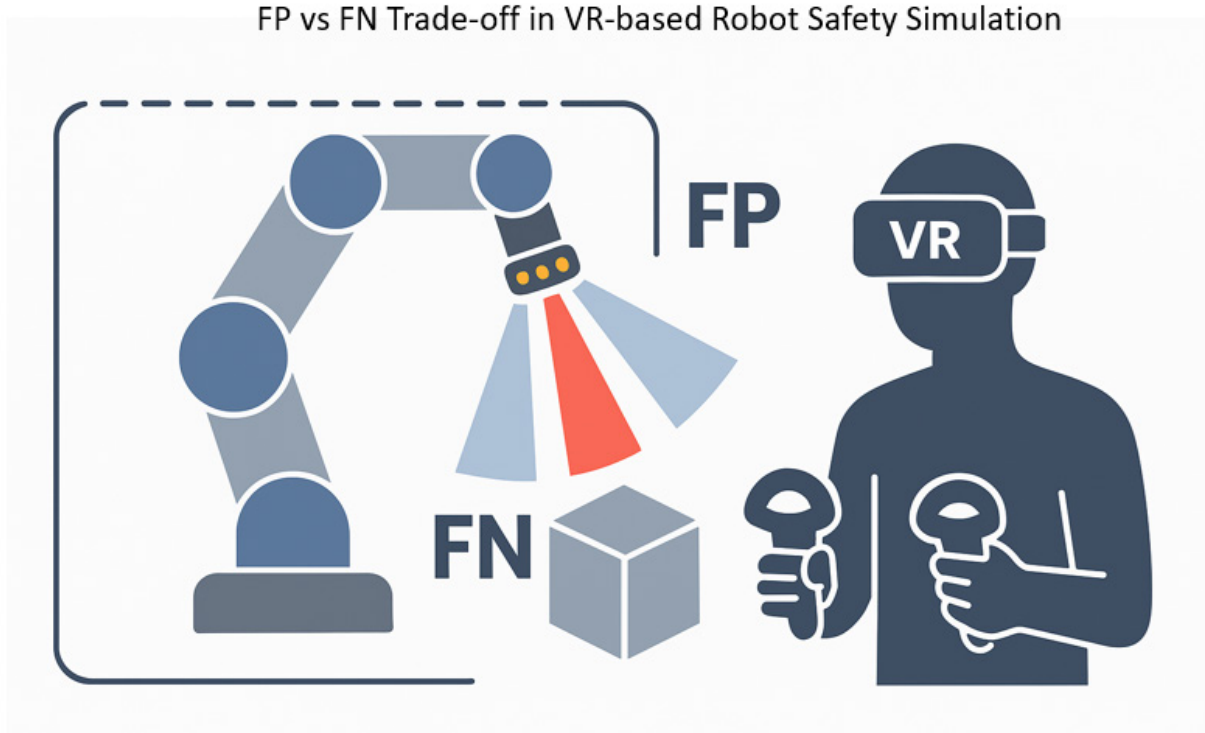

doi: 10.25100/iyc.v27i2.14759

Introduction

The Fourth Industrial Revolution (4IR) has driven significant transformations in the manufactur- ing industry through the adoption of advanced technologies such as the Internet of Things (IoT), Big Data, Artificial Intelligence (AI), the cloud, and robotics. These advancements have facili- tated the development of smarter, more interconnected, and highly flexible production systems, enabling real-time monitoring, optimization, and adaptation of processes to meet the demands of increasingly dynamic markets (1, 2).

Within the framework of the 4IR, a prominent trend is the integration of collaborative manufac- turing approaches, which synergize automation with human expertise to enhance operational flexibility and efficiency. This evolution has been further accelerated by the implementation of cyber-physical systems and IoT, which establish seamless connections between physical as- sets—such as robots and machines—and digital data streams. These technologies have laid the foundation for effective collaboration between humans and robots in manufacturing environ- ments (1, 2).

In this context, collaborative robots, or cobots, have emerged as fundamental enablers of these advancements. Unlike traditional industrial robots, which operate in isolation, cobots are en- gineered to safely interact with human operators, sharing tasks and leveraging their respective strengths. This paradigm shift addresses the growing need for production systems capable of adapting to mass customization and reduced lead times, while upholding rigorous safety stan- dards (2). Nevertheless, collaborative environments also introduce significant challenges, par- ticularly in ensuring effective human-robot interaction (HRI). This requires robots not only to prevent collisions but also to engage intentionally in collaborative tasks, such as tool exchanges and co-assembly (3, 4).

In manufacturing environments, time is optimized while meeting strict human safety stan- dards. To date, the most effective safety method has been the spatial separation of humans and robots (5). However, to enable effective collaboration, it is necessary to eliminate this sep- aration through systems that not only prevent collisions (3) but also allow intentional contacts, such as tool exchanges (4).

Current collision avoidance systems in collaborative manufacturing environments incorporate a wide range of approaches designed to ensure safe and efficient interaction between humans and robots. These systems consist of object proximity detection sensors and trajectory planning algorithms that collaborate to prevent collisions in real-time and dynamically adapt to environ- mental changes (6, 7, 8).

In terms of sensors, collision avoidance systems (9) may employ force sensors, ultrasonic sen- sors (10), infrared time-of-flight (ToF) sensors (11), and depth cameras. Regarding the latter technology, studies such as (12, 13, 6, 14, 15) use two or more cameras to recognize the envi- ronment through point clouds, generating 3D images or scene recognition. These sensors are integrated into the robot, operator, or environment to detect and measure the position, speed, and acceleration of objects and people (16, 17). Collision avoidance in HRI environments de- mands sophisticated

doi: 10.25100/iyc.v27i2.14759

methods (8) that merge data from multiple sensors (radars, infrared, laser) to leverage the strengths of each technology (18).

One of the main barriers to adopting collaborative robots in manufacturing environments is the excessive time required to configure the sensor networks that integrate the collision avoidance system (19). When this configuration is performed through trial and error on the real prototype, multiple trials are required under strict protocols to ensure user safety. To address these challenges, the concept of a digital twin is introduced. A digital twin is a virtual representation of the physical robot and its environment, used to simulate sensor configurations, collision avoid- ance strategies, and task dynamics. This approach reduces the time and costs associated with physical experimentation and improves the evaluation and adjustment of collision detection systems.

The significant time investment, high costs, and safety risks involved in configuring physical sensor systems have driven the adoption of innovative alternatives such as virtual reality (VR). VR provides a realistic and controlled simulation environment that enables users to interact with sensor configurations and test collision avoidance algorithms without exposure to real-world hazards. Its integration into manufacturing processes not only enhances safety and operational efficiency but also supports the evaluation and optimization of sensor arrangements, helping to prevent adverse events in collaborative human-robot environments (20, 21).

This research addresses collision avoidance in collaborative manufacturing environments (18) through the development of a VR system that simulates the effect of different spatial arrangements of ultrasonic and infrared sensors in preventing collisions between the operator and the robot. During the execution of the manufacturing task in the virtual environment, the user employs the Meta Quest II device to provide the positions of the hands, which are tracked and replicated in the virtual environment as an avatar. The avatar interacts with the simulation, al- lowing the sensors on the robot to detect its presence and movement, facilitating the evaluation of sensor configurations.

In this context, the present study develops a VR simulator using Unity3D and URSim to evaluate and optimize configurations of ultrasonic and infrared sensors in collaborative robots. This sim- ulator allows experimentation with key sensor parameters, such as detection distance, dispersion angle, sampling frequency, and noise level, providing a controlled environment to replicate and analyze sensor behaviors. While not a replacement for physical testing, the simulator serves as a cost-effective and efficient tool to previsualize and validate sensor layouts and parameters, offering insights into their expected performance and behavior before physical implementation. This approach significantly reduces the time, costs, and risks associated with traditional trial- and-error testing on real prototypes.

Related Works

The optimization of physical sensors and the use of VR in HRI represent significant advance- ments in collaborative robotics. This section reviews relevant research on these topics, address- ing sensor technologies and their integration into collaborative systems through VR.
Research on proximity sensors has focused on the integration of piezoresistive, capacitive, and

doi: 10.25100/iyc.v27i2.14759

ultrasonic technologies to improve detection in collaborative environments. Flexible and cost-effective solutions for curved surfaces and diverse materials have been explored, as demon- strated in the work of Fonseca (22) and Tong (10). Wu et al. (23) proposed geometric models to optimize sensor placement while minimizing resources without compromising coverage.

Innovative designs such as a dual-mode sensor based on inductive and capacitive principles have been introduced, as described by Nguyen (24). Trends in proximity technologies, including method combinations and advancements in data processing, were identified in a review by Xing (25). Tsuji and Kohama(26) proposed a modular system that combines time-of-flight (ToF) and self-capacitance sensors for continuous proximity and contact detection.

In the domain of VR, its application in the simulation and validation of collaborative worksta- tions has been explored to optimize cycle times and layout designs, as discussed by Malik (27).

Worker-centered design in collaborative systems has been evaluated through VR, as highlighted by Aschenbrenner (28). The applications of VR in HRI, particularly in communication and re- mote collaboration, were reviewed by Lei (9). Virtual environments have also been shown to reduce mental workload in complex collaborative tasks, as examined by Nenna (29).

The combination of digital twins and VR has enabled the design and evaluation of worksta- tions, integrating simulations to analyze ergonomics and safety, as demonstrated by Havard (30). CushSense, a stretchable tactile skin designed for dynamic human-robot interaction, was developed by Xu (31). Additionally, a framework for anticipating contacts using capacitive sensors was proposed by Escobedo (32), optimizing the transition between avoidance and in- tentional contact.

These studies highlight advances in physical sensor technologies and VR as complementary tools for simulating, validating, and designing collaborative systems. The integration of these technologies facilitates the creation of safer, more efficient, and user-centered work environ- ments.

Background

Safety in human-robot interaction within collaborative environments can be categorized into collaborative, coexisting, and assisted interactions, each presenting distinct safety challenges. Collaborative interactions demand highly accurate collision detection systems due to the con- stant proximity between humans and robots. In coexisting interactions, where humans and robots share the same space but perform different tasks, the primary safety concern is prevent- ing unintentional intersections of their paths. Assisted interactions require precise coordination between robot actions and human movements to avoid accidental collisions. The critical need for reliable detection systems is underscored by industrial accidents, highlighting the necessity of ensuring both safety and operational efficiency (33).

Object proximity detection sensors

In collaborative manufacturing, collision detection between humans and cobots is essential for maintaining a safe and efficient environment. Various methods exist for this detection, includ- ing vision-based sensors such as RGB cameras and image analysis with artificial intelligence, internal

doi: 10.25100/iyc.v27i2.14759

sensors within the cobot that use readings from the cobot itself, such as torque (22, 34), and sensors based on tactile and proximity technologies, integrated into the cobot's structure (UR3, KUKA).

Vision-based sensors, while effective, face challenges such as occlusion, changing light condi- tions, shadows, sensor device vibration, and the need for multiple cameras to cover all possible angles (35, 36). Occlusion, where objects obstruct the sensor's line of sight, can lead to in- complete or inaccurate point clouds, resulting in gaps in the 3D model. Additionally, these sensors are sensitive to lighting conditions; low light can reduce the signal-to-noise ratio, and excessive brightness can cause overexposure, both of which impair depth detection. Shadows can also create false depth cues, confusing the sensor's interpretation of the scene, while sensor vibrations may misalign captured frames, distorting the 3D reconstruction (35, 36).

For sensors that generate point clouds or depth maps using infrared technology, similar challenges arise. Occlusion can block the infrared beams, leading to incomplete data capture. Infrared interference from other sources can degrade depth accuracy, while surface reflectivity—particularly on highly reflective or transparent surfaces—can cause errors in measurement. Additionally, environmental noise, such as dust or mist, can scatter infrared rays, reducing the clarity of the data. These issues not only affect the depth accuracy but also complicate the generation of point clouds used for three-dimensional scene recognition, potentially leading to gaps or inaccuracies in the 3D model. These factors collectively impact the sensor's ability to provide accurate and reliable data in real-world conditions (12, 13, 6, 14, 15, 37).

In contrast, tactile and proximity sensors—such as capacitive, ultrasonic, or short-range in- frared—are designed for close-range detection and serve a fundamentally different purpose than infrared-based depth mapping systems. While depth cameras and similar systems aim to reconstruct detailed 3D environments over medium or long distances, proximity sensors focus solely on detecting the presence of nearby objects or humans, without the need to identify their shape or spatial structure. Because they do not rely on visual input, these sensors are unaffected by occlusion, lighting conditions, or environmental shadows. Ultrasonic sensors, although lim- ited in range, perform reliably in low-visibility environments and are less affected by surface reflectivity (10, 11). Similarly, short-range infrared sensors use the time-of-flight (ToF) of light to detect close objects and maintain consistent accuracy even in the presence of dust, dirt, or other interfering particles (11). Despite these advantages, such sensors also present certain limitations. Ultrasonic sensors may experience interference when multiple devices are used simultaneously and cannot detect soft materials that absorb acoustic waves. Infrared sensors may have issues with light scattering on curved surfaces, affecting their resolution and accuracy. Furthermore, implementing both types of sensors in hardware systems can be complicated due to irregularities in the device structure, making proper integration challenging. The main drawback lies in the process of reconfiguring, adapting, and repositioning the sensors on the hardware, especially when multiple patterns need to be tested to find the optimal configuration (14, 22).

VR simulation

VR offers a promising solution to challenges in collaborative manufacturing related to the experimentation in improving collision avoidance (9). VR simulation environments allow the creation

doi: 10.25100/iyc.v27i2.14759

and testing of various sensor configurations without the risks and costs associated with physical experimentation. In a virtual environment, typical physical sensor issues, such as visual obstructions, environmental conditions, and external factors, are eliminated (20, 21). VR provides a controlled setting that facilitates accurate and consistent evaluation of sensor configurations. VR simulation facilitates the identification and evaluation of optimal sensor configurations, pro- viding a basis for implementing safe and efficient solutions in real environments. It also avoids the need to repeatedly relocate, reposition, and disassemble sensors during the testing process, saving time and resources. A digital twin, which is a virtual representation of the physical cobot, replicates the robot's structure and behavior within the virtual environment. This virtual model allows for performance evaluation and determination of the most suitable configuration before physical implementation (38, 7). This approach optimizes safety and operational efficiency in collaborative manufacturing, reducing the costs and risks associated with physical experimen- tation, as highlighted in (39, 40, 41, 42). The ability to make adjustments and conduct tests in a controlled virtual environment enables rapid and precise iterations, improving the efficiency of the design and implementation of detection systems.

Materials and methods

The simulation environment is executed on a high-performance workstation equipped with an i7-12700H processor, RTX 4070 graphics card, and 32GB of RAM. This setup mitigates common issues associated with VR environments, such as motion sickness, visual fatigue, spatial disorientation, and latency failures, which can significantly impact user experience and usabil- ity (43). The virtual environment is optimized for execution on the Meta Quest II, with improve- ments in meshes, textures, and code to ensure smooth operation and adequate performance.

The proposed system is modular and consists of three main components, as illustrated in Fig- ure 1, which provides a visual representation of how the user interacts with the simulation system. The components are: (1) a motion capture system based on the Meta Quest II device, which tracks the user's hand positions and replicates them as an avatar in the virtual environ- ment; (2) a digital twin of the UR3 robot, visualized and controlled through Unity3D, enabling interaction between the robot and its virtual surroundings; and (3) a virtual machine running URSim, which contains the mathematical models that define the kinematics and dynamics of the robot. The Figure 1 summarizes the key elements of the simulator and their roles in sup- porting user interaction and simulation tasks.

This modular setup enables the system to perform real-time testing and evaluation in a safe, virtual environment. Specifically, the simulation was designed to assess different spatial ar- rangements and functional parameters of proximity sensors—modeled to emulate ultrasonic and infrared behavior—within a collaborative assembly task where a robotic arm delivers parts to a human operator. For simplicity, each sensor is represented as a flat cylindrical element ("button") attached to the robot surface. The physical dimensions and form factor of the sensor are not considered in this study, as the focus lies on sensing behavior rather than mechani- cal integration. Each sensor emits multiple rays in a conical pattern, projected outward along the sensor's surface normal, using Unity's raycasting system to simulate proximity detection. Users can configure key

doi: 10.25100/iyc.v27i2.14759

parameters such as the maximum detection distance, the cone's dis- persion angle (Figure 2), sampling frequency, measurement noise, and the number of emitted rays. These parameters are varied to replicate the behavior of different sensor types and serve as experimental factors in the evaluation described in Section 4.6.

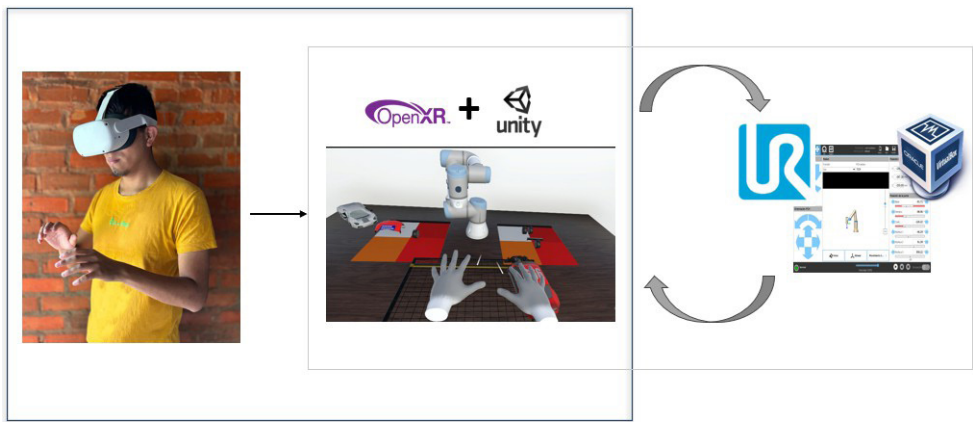

Figure 1. Overview of the data flow between the user (VR), Unity simulation, and URSim virtual controller.

Figure 1 illustrates the interaction flow within the simulation system, and each of its elements is described as follows. On the left side of the figure, the user is shown wearing a Meta Quest II headset and interacting through natural hand movements, which are captured via integrated hand-tracking. In the center, the Unity 3D engine processes these inputs through the OpenXR framework, allowing the user to control a virtual avatar that manipulates objects and interacts with the digital twin of the UR3 robot. On the right, the URSim simulator is depicted, which receives motion commands from Unity and returns execution data for synchronized robot be- havior. The bidirectional arrows indicate the real-time flow of information between Unity and URSim, representing a continuous feedback loop within the simulation environment.

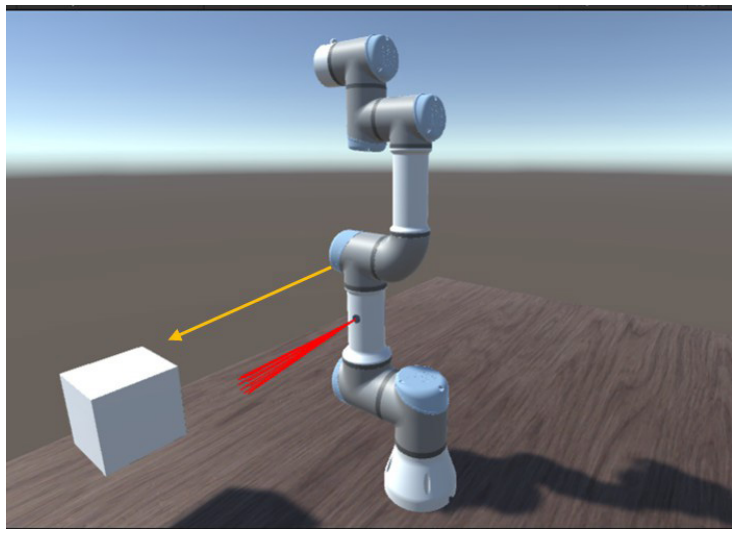

Figure 2. Detection cone of distance sensors

doi: 10.25100/iyc.v27i2.14759

Robot controller

URSim handles the robot's movement logic using TCP/IP communication. The controller, in version 5.13.1, runs under a virtual machine on the same workstation. URSim sends and re- ceives commands to Unity3D, ensuring precise synchronization of movements. Inverse kine- matics, calculated by URSim, allows the execution of defined movements for the robot. This integration enables the robot to perform programmed tasks, such as pick-and-place movements, in the simulated environment. The base project used for this communication is taken from the GitHub repository [1].

Digital twin and VR environment

The 3D models and textures of the UR3 digital twin were imported from Blender and rendered in the development engine, which handles real-time graphics and physical simulations. The dig- ital twin, executed in Unity3D, operates based on sensor configurations and control commands received from URSim. The robot's trajectory—from origin to destination—is defined using spherical interpolation for smooth rotational transitions and linear interpolation for straight-line motion in 3D space. If an obstacle is detected along the path, the robot performs a preventive stop to avoid collisions, without discarding or recalculating the original trajectory. The desti- nation remains defined, and movement can resume once the obstruction is no longer present. Scripts interpret these commands and update the joint positions and actions of the robot's end effector in the virtual environment.

Data storage

During each simulation session, sensor data is continuously collected and monitored. The data storage frequency is adjusted according to the sampling frequency configured for each sensor, ensuring precise correspondence between data collection and sensor configuration. At the end of the test, this data is saved in two Javascript Object Notation (JSON) files: one contains the static data regarding the sensor configuration and the test name, and the other stores the dynamic data from the beginning to the end of the test. The sensors record all the information presented in Table 1 during each reading, which includes details such as object detection time, speed, position, and collision events. While the system logs individual collision events with full object-level details, the analysis primarily focuses on the total number of collisions per test as a global indicator of sensor performance. This aggregate metric is later used to categorize events into direct collisions, undetected collisions, and successful evasions, enabling a more nuanced interpretation of each sensor configuration's behavior.

doi: 10.25100/iyc.v27i2.14759

Table 1: Description of the variables used in the simulation

Variable Name	**Description**
Name of the object	Identifier of the detected object in the simulation.
Detection time	Exact detection moment in the simulation, based on the sensor's sampling rate.
Object speed	Speed at which the detected obstacle approaches or moves away from the sensor.
Position relative to the base	Object's location relative to the robot's base.
Orientation in virtual plane	Rotational alignment of the object in the virtual environment.
Number of obstacles detected	Counts objects within the sensor's detection range as obstacles.
Total collisions	Number of collisions between the robot and any object.

System architecture overview

Figure 3 provides a comprehensive overview of the system architecture, highlighting the interaction and data flow between its main components. This design is organized into three interconnected levels. At the upper level, the user, through the Meta Quest II device, interacts with the system by translating their movements into digital commands processed within the virtual environment. At the intermediate level, Unity 3D manages the digital twin of the UR3 robot, integrating real-time sensor configurations and visualizing the robot's movements. Unity also continuously evaluates the data captured by the sensors, such as object detections, prox- imity events, and critical conditions, and, if necessary, sends instructions to URSim to stop the robot's movement as part of a safety mechanism. In parallel, URSim, located at the lower level, calculates the robot's movements based on the received instructions and sends information back to Unity about the robot's state and executed movements, allowing them to be replicated in the digital twin. Additionally, Unity stores key information in JSON format: static data comprising the initial sensor configurations and dynamic data recorded during the simulation. This modular architecture ensures a continuous and coordinated flow of information, optimizing the evalua- tion of sensor configurations and detection strategies in a safe and controlled environment.

doi: 10.25100/iyc.v27i2.14759

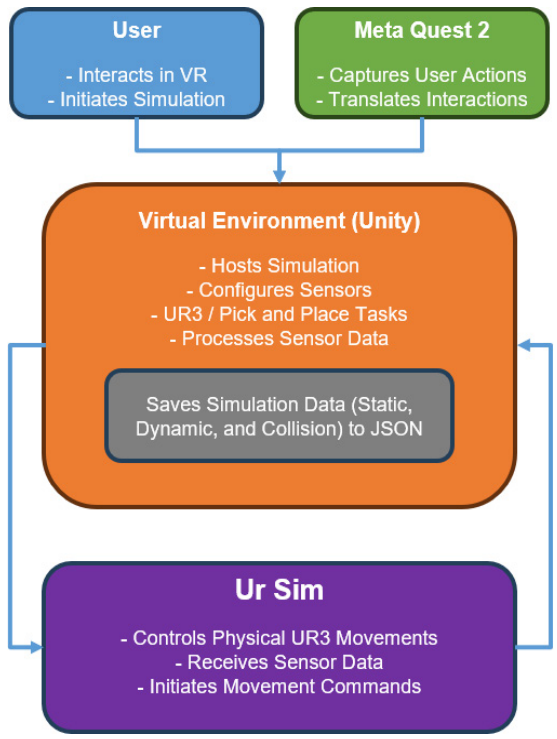

Figure 3. System architecture diagram

Simulation environment

The experimental setup was designed to simulate a collaborative workspace where the user and the robot share a defined interaction space. Figure 4 illustrates the spatial layout of the environment through two complementary views. Subfigure (a) provides a schematic represen- tation of the key zones involved in the interaction: the object zones located at the corners, the delivery zone shared between the user and the robot, and the robot's movement zone at the cen- ter. Subfigure (b) shows the same distribution of zones rendered within the Unity simulation environment, allowing a clear correspondence between the conceptual layout and its implemen- tation. To provide a broader understanding of the simulation context, Figure 5 presents an overall perspective of the virtual environment. This includes a typical workbench setting where pick-and-place tasks are performed, the position of the robot on the table, and the surrounding space where the user interacts. This view helps contextualize the spatial arrangement shown in Figure 4, offering insight into the visual and functional aspects of the simulated collaborative workspace.

doi: 10.25100/iyc.v27i2.14759

(a) Schematic layout (b) Top-down view in Unity

Figure 4. Workspace zones. (a) Conceptual layout showing the robot, object, and delivery zones. (b) Unity representation of the same spatial zones.

Figure 5. General view of the virtual collaborative environment developed in Unity, showing the robot's position and the surrounding work area for the user.

System interaction and configuration

Upon starting the simulator, the user is presented with a user interface (UI) featuring a start button. The UI is structured to allow the user to navigate through the available options. The UI offers two main options: manually creating sensors or loading saved configurations.

In the manual creation option, the user can place sensors by directly touching the surfaces of the robot's joints. This tactile interaction allows precise control over the sensor locations. Additionally, the UI allows for adjusting the height and rotation of each sensor. Sensor configuration includes selecting the type of sensor (ultrasonic, infrared, or custom), as well as the ability to save configurations for future testing (Figure 6).

doi: 10.25100/iyc.v27i2.14759

Preset configurations are provided to simulate the behavior of ultrasonic and infrared sensors, and there is also the possibility to create custom sensors with specific characteristics according to the user's needs. Sensors placed on the joints can vary in height and rotation on the joint where they are generated, providing greater control and precision in detection.

This functionality facilitates the repeatability of tests and the optimization of sensor configurations. The capability to store up to three different configurations allows users to directly compare the performance of various sensor arrangements under similar test conditions. With the sensors configured and loaded, the user initiates the simulation, where the robot awaits the TCP/IP connection to establish communication with URSim. This connection is essential for synchronizing the robot's movements in the virtual environment with the real control logic.

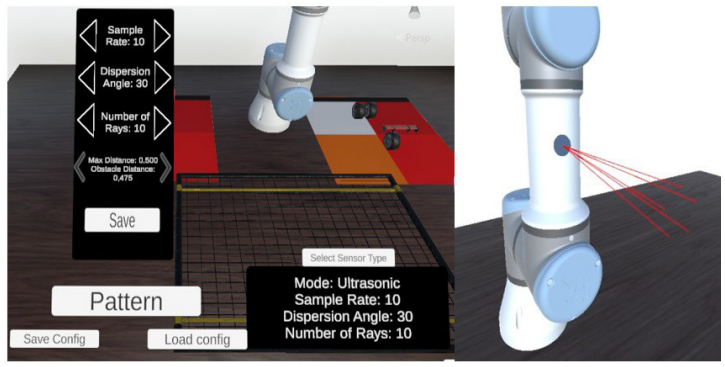

Figure 6. User interface for sensor configuration

Although this interface supports interactive sensor creation and configuration, the experiments presented in this work were designed to use preloaded parameter files to ensure consistency and reproducibility. Nevertheless, the manual configuration functionality remains essential for future testing scenarios and exploratory evaluations involving alternative sensor characteristics or placements.

Simulation operation and results

Once the connection is established, the robot moves to a base position, and a green light indicates it is operational and ready to pick the next part. During the simulation, the robot identifies the location of the part to be picked, calculates the optimal path to reach it, moves to the specified position, and executes the programmed action to securely grasp and retrieve the part. After completing this task, the robot transports the part to the designated drop-off location and releases it according to its programmed routine. Each movement and action is monitored in real- time, allowing the user to observe how the sensors detect objects and how the robot responds to these stimuli.

The simulation provides visual and auditory feedback to enhance observation and evaluate the robot's performance. A green light indicates that the robot is ready to operate and pick the next part. If a sensor detects an object within its range, a yellow light signals a precautionary warning,

doi: 10.25100/iyc.v27i2.14759

the robot sends a stop command to prevent a collision, and an intermittent sound alerts the user. In the event of a collision, a red light highlights the impact, evidencing whether the robot successfully avoids or collides with an object.

Detailed data on sensors and their detections are recorded throughout the simulation. At the end of the test, a report summarizing the collected data is automatically generated. This information enables the evaluation of sensor performance and facilitates adjustments to configurations, improving the system's ability to prevent collisions.

Predefined sensor arrays

In the review of studies addressing safety in collaborative robots and strategies for collision prevention (3, 9, 44), as well as those focused on the development or testing of novel tactile and proximity sensing systems, three predominant sensor configurations were consistently identi- fied. These configurations are defined not only by the type of sensor used, but primarily by their spatial distribution and intended sensing coverage. The first, referred to as the 360-degrees configuration, involves the placement of sensors around the circumference of the robot's main joints to achieve omnidirectional proximity awareness—this approach appears frequently in systems designed for full-surface monitoring. The second, known as the End-joint skin config- uration, concentrates sensors around the wrist and terminal joints—those closest to the gripper or tool—where most physical interaction with objects or humans typically occurs. The third configuration consists of Lateral sensor placements along key joints (e.g., elbow or shoulder), covering the sides of the robot's kinematic chain to enable monitoring of approach angles with- out requiring full coverage. Although the specific sensor types and placements vary between studies, these three configurations represent common patterns in the literature. In this work, representative versions of each configuration were implemented in a standardized simulation environment using a UR3 digital twin (Figure 7).

In this study, these configurations are emulated using the simulator and evaluated in a standard- ized environment with a digital twin of the UR3 robot (Figure 7). Given that the cobot models in the original studies vary, these configurations were adapted to the digital twin model of the UR3 to standardize testing conditions. The identified configurations are as follows:

360-degrees. Sensors are arranged at a 360-degree angle around joints two, three, and six, providing detection in all directions (Figure 7a). This arrangement allows the robot to identify obstacles from any direction around its main joints, which is essential to avoid collisions during movements in dynamic environments (45, 31, 46, 47).

End-joint. Complete sensor coverage on joints four, five, and six, focusing on areas of direct interaction with the environment (Figure 7b). This configuration maximizes detection in critical areas for object manipulation, allowing precise responses to contact and proximity (26, 11, 22, 24, 48).

Lateral Sensors are arranged laterally on joints two and three, with two sensors on each side, and three sensors on the final joint, oriented to the sides and front (Figure 7c). This arrangement is the most common for covering the main joints and allows the robot to have extended lateral vision (49, 32, 23, 50).

doi: 10.25100/iyc.v27i2.14759

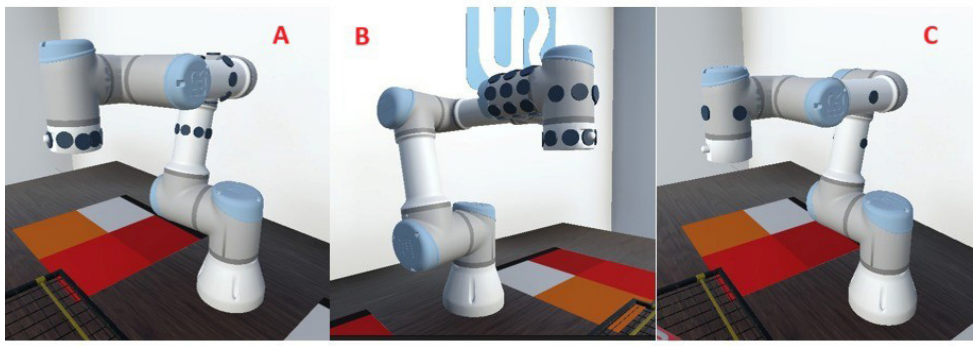

Figure 7. Sensor configurations: (a) 360-Degree distribution on main joints, (b) End joint skin, (c) Lateral sensors on main joints

Experimental Design

The three sensor configurations introduced in Section 4.5— 360-degrees, End-joint, and Lat- eral as the basis for evaluating sensor behavior under multiple parameter combinations. As previously described, each sensor is simulated as a flat cylindrical element emitting rays in a conical pattern along its surface normal, with configurable properties such as Distance, Angle, Sampling, and Noise. The number of emitted rays per sensor was kept constant throughout the experiments to isolate the effects of the tested parameters.

The following five input factors were varied during the experiments:

Maximum detection distance (D_{max}). Tested at three levels (15 cm, 30 cm, and 50 cm), representing the maximum range at which the sensors can detect an object.

Dispersion angle (A_d). Evaluated at two levels (4° and 25°), this factor defines the angular aperture of the sensor's detection cone. A smaller A_d provides more focused detection, reducing false positives, while a larger A_d increases the area covered but may lead to more irrelevant detections.

Sampling frequency (T_m). Tested at two levels (10 Hz and 100 Hz), T_m indicates the interval between consecutive sensor readings. Higher T_m (faster sampling) allows for quicker reaction times but may increase processing demands.

Noise level (N). Representing real-world interference, noise was tested at two levels (2% and 5%). Higher noise levels are expected to challenge the sensors' ability to distinguish obstacles from background signals.

Sensor configuration. This factor includes the three spatial layouts (360-degree, end joint, and lateral) defined in Section 4.5.

Sensor performance was evaluated using the following response variables:

False positives (FP). Instances where the sensors detected objects that were not actual obstacles.

False negatives (FN). Cases where a collision occurred because the sensors failed to detect the object. The experiment was designed to test all possible combinations of the five factors listed above. Each parameter combination was repeated three times to ensure statistical robustness. The total number

doi: 10.25100/iyc.v27i2.14759

of tests was calculated as follows:

$$\text{Total Tests} = 3 \text{ configurations} \times (3 \text{ levels of } D_{max}) \times (2 \text{ levels of } A_d) \times (2 \text{ levels of } T_m) \times (2 \text{ levels of } N) \times 3 \text{ repetitions} = 216 \text{ tests.}$$

These 216 tests encompassed 72 parameter combinations, each repeated three times to account for variability and ensure measurement accuracy and comparability between tests. The se- quence of the tests was randomized to prevent systematic biases and ensure robust results. Additionally, the system was executed in an automated manner to eliminate variability intro- duced by human intervention. Unlike a manual test with a user in the simulated environment, where variations in timing and movements may occur, automation ensures that each repetition is conducted under identical conditions.

Static objects were placed at predefined positions within the robot's environment. In each test, three objects were strategically positioned along the robot's trajectory, with one at each phase of movement: picking, placing, and returning. These objects appeared at predefined times within each movement interval, allowing for the evaluation of parameter impacts without uncontrolled interferences or modifications. Figure 8 illustrates these phases, labeled as a) (picking), b) (placing), and c) (returning).

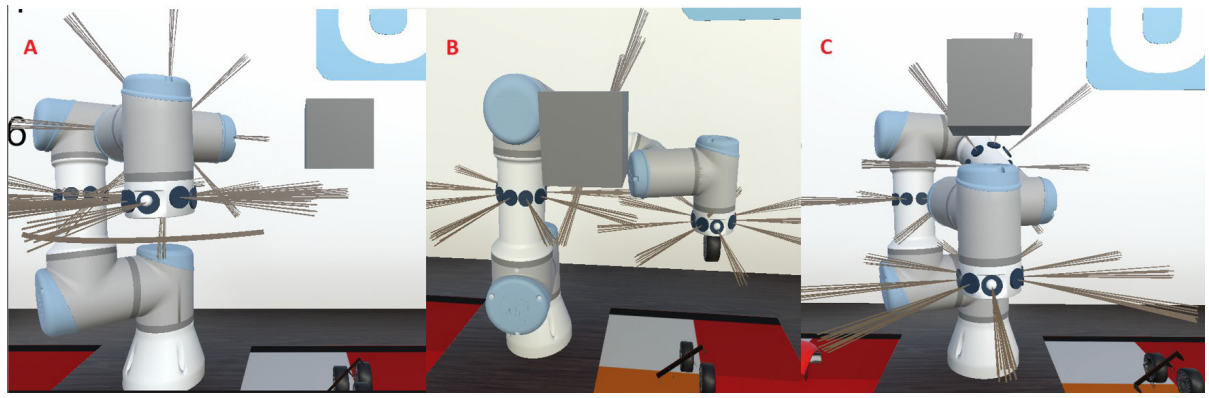

Figure 8. Illustration of the three movement phases in the automated test. Subfigure a) corre- sponds to the picking phase, b) to the placing phase, and c) to the returning phase.

While the automated tests ensured consistent and repeatable conditions, they did not account for the variability introduced by human presence in the workspace. To address this limitation, a second experiment was designed involving user participation within the same environment.

Second Experiment: User-based Evaluation

This experiment incorporated user interaction into the pick-and-place scenario to evaluate how sensor behavior was influenced by human presence and movement in the shared workspace. During this stage, the user assembled a vehicle using the components provided by the robot. Additionally, to increase the level of interaction within the shared workspace, a complemen- tary

doi: 10.25100/iyc.v27i2.14759

activity was introduced: secondary pieces—distinct from those used in the vehicle assem- bly—appeared randomly in a designated Zone A (on the left or right side of the table), and the user was required to transport them to Zone B on the opposite side. This action ensured that the user's movements intersected with the robot's workspace, promoting conditions in which the sensors could register potential interactions (Figure 9).

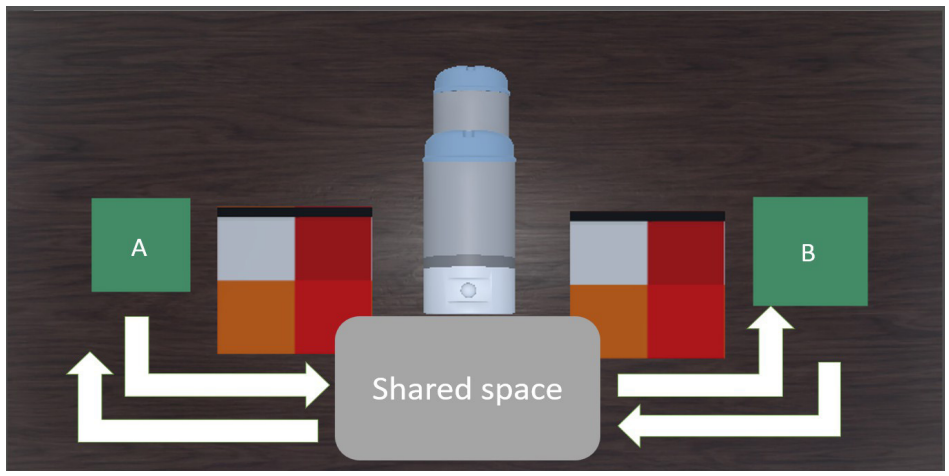

Figure 9. Zones A and B used during the secondary transport activity. Objects appear randomly in either Zone A or Zone B, and the user is required to transport them to the opposite zone, crossing the shared space with the robot in the process.

To prevent user behavior from being influenced by the sensor layout used in each condition, both the visual projection of the detection areas and the visibility of the physical sensors were concealed. This measure ensured that neither the presence of laser beams nor the physical place- ment of the sensors acted as visual references that could influence the user's behavior during the task. The intention was to avoid instinctive avoidance behavior or deliberate trajectory modi- fications that could compromise the natural flow of interaction within the shared workspace (Figure 10).

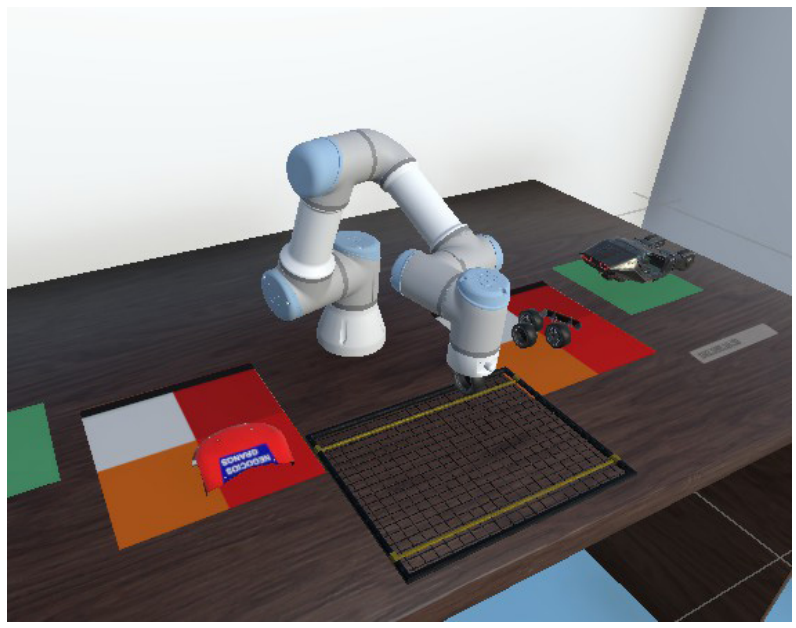

Figure 10. User view without visible sensor rays or elements.

doi: 10.25100/iyc.v27i2.14759

To further standardize the conditions, the user was instructed to transport the objects along a predefined central route and at a medium height across the table. This constraint ensured consis- tent overlap with the robot's operational area and the corresponding detection zones, increasing the likelihood of registering proximity events during the movement. The configuration was de- signed to emulate plausible interaction scenarios while ensuring that the detection mechanisms could be consistently triggered.

The experimental design for this stage included two distinct parameter combinations, summa- rized in Table 2. Each combination was tested under the three sensor layouts (360-degrees, End-joint, and Lateral), with four repetitions per condition. As in the automated test, the anal- ysis focused on the detection outcomes: FP, and FN.

Table 2. Parameter combinations used in the user-based experiment

	CombinationD_{max} (cm)	A_d (°	T_m (Hz	N
A	30	25	100	0.05
B	15	4	10	0.02

The number of tests carried out in this stage is defined as:

Total Tests = 2 combinations × 3 configurations × 4 repetitions
= 24 tests.

Statistical Analysis Methods

To evaluate the performance of the different sensor configurations and factor levels, the follow- ing statistical methods were applied to both tests:

Analysis of variance (ANOVA). Used to determine whether variations in the experimental factors (distance, angle, sampling frequency, noise level, and sensor configuration) had a significant effect on the response variables.

Shapiro-Wilk test. It is conducted to verify whether the data follow a normal distribution, which is a key assumption for ANOVA.

Levene's test. It assesses whether the variance of the response variable is equal across the groups formed by all possible combinations of factor levels. If the null hypothesis is rejected the data are not homocedastic, which indicates that the variability of the response differs among at least two of these groups.

Tukey's honestly significant differences. These are statistical tests conducted after a sig- nificant effect is detected in an ANOVA test. These post-hoc tests help identify which specific levels differ when a factor or interaction effect is significant.

doi: 10.25100/iyc.v27i2.14759

Results

First Experiment: Automated Evaluation

This section presents the statistical analysis of an experiment that examined the effects of the five factors described in Section 4.6 (Distance, Angle, Sampling, Noise, and Setup) on two response variables (FP and FN). The analysis includes tests for assumptions, main effects, fol- lowed by post-hoc comparisons. Table 3 summarizes the verification of ANOVA assumptions for each response variable.

Table 3. ANOVA assumption verification for the response variables

Variable	Test	p-value	Significant
FP	Normality	≤ 0.001	TRUE
FP	Homoscedasticity	0.6171	FALSE
FP	Independence	0.3270	FALSE
FN	Normality	≤ 0.001	TRUE
FN	Homoscedasticity	0.5483	FALSE
FN	Independence	0.0880	FALSE

Although the residuals of the ANOVA models for FP and FN did not meet the normality as- sumptions ($p \leq 0.001$), the analysis remains valid due to the robustness of ANOVA to devia- tions from normality, particularly when the assumptions of homoscedasticity and independence are satisfied (51). Table 3 shows that both models passed the Levene's test, confirming homo- geneity of variances across groups, and the Durbin-Watson test, ensuring the independence of residuals. Given these two conditions, the ANOVA results can be interpreted reliably despite the non-normality of residuals. Furthermore, previous research suggests that normality devia- tions have a negligible impact on Type I error rates when group sizes are balanced and sample sizes are moderate to large. The results for the FP and FN response variables are presented in Table 4. For both response variables, only the factors Distance, Angle, and Setup exhibited statistically significant effects ($p < 0.05$).

Table 4. Significance of the main factors on the FP and FN response variables

Factor	p-value (FP)	p-value (FN)
Distance	≤0.001	≤0.001
Angle	≤0.001	≤0.001
Sampling	0.570	0.269
Noise	0.631	0.874
Setup	≤0.001	≤0.001

The post-hoc contrasts for the FP variable are presented in Table 5. The first row indicates a positive difference in the average number of FP obtained between the detection distances of

doi: 10.25100/iyc.v27i2.14759

30 cm and 15 cm. The second row is consistent with this finding, suggesting that as the maximum detection distance of the sensor increases, the number of FP also increases. However, no significant differences in the average number of FP were found between the 30 cm and 50 cm detection distances. The fourth row shows that a greater angular aperture of the sensor's detection beam corresponds to a higher number of FP. Regarding the effect of sensor layout, the 360-degrees configuration exhibited the highest number of FP, followed by the End-joint configuration. Hence, the lateral sensor array resulted in the lowest number of FP.

Table 5. Post hoc contrast tests for the response variable FP

Factor	**Contrast**	**Estimate**	**p-value**
Distance	30 cm - 15 cm	77.458	≤0.001
Distance	50 cm - 15 cm	78.694	≤0.001
Distance	50 cm - 30 cm	1.236	0.987
Angle	25° - 4°	82.102	≤0.001
Setup	End-joint- 360-degrees	-53.375	≤0.001
Setup	Lateral- 360-degrees	-247.639	≤0.001
Setup	Lateral- End-joint	-194.264	≤0.001

The post-hoc contrasts for the FN variable are presented in Table 6. The first two rows of Table 6 indicate that the behavior of FN with respect to the maximum sensor distance differs from that of FP. Specifically, for FN, a detection distance of 15 cm results in the highest number of FN. However, despite the statistical significance of these differences, their magnitude is relatively small, averaging around 1 FN. This is a very low value compared to the differences in the number of FP observed in Table 5. The Angle factor also exhibited the opposite effect compared to FP: a greater angular aperture of the sensor's detection beam corresponds to a lower number of FN. Regarding the effect of sensor arrays, only the End-joint configuration showed significant differences compared to the other two configurations. This configuration had the lowest number of FN, differing on average by six FN.

Table 6. Post hoc contrast tests for the response variable FN

Factor	**Contrast**	**Estimate**	**p-value**
Distance	30 cm - 15 cm	-1.083	≤0.001
Distance	50 cm - 15 cm	-1.042	≤0.001
Distance	50 cm - 30 cm	0.042	0.954
Angle	25° - 4°	-1.130	≤0.001
Setup	End-joint- 360-degrees	-6.086	≤0.001
Setup	Lateral- 360-degrees	-0.153	0.536
Setup	Lateral- End-joint	6.653	≤0.001

The boxplots in Figure 11 illustrate that the Lateral setup minimizes the number of FP, while the End-joint configuration leads to lowest number of FN.

doi: 10.25100/iyc.v27i2.14759

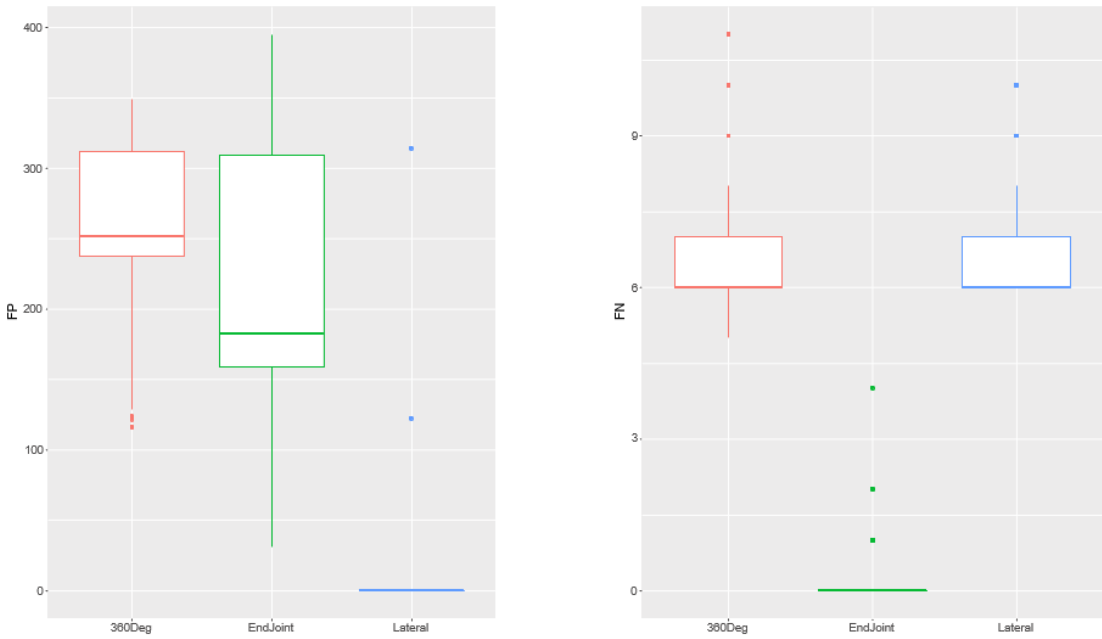

(a) FP as a function of the sensor *Setup*

(b) FN as a function of the sensor *Setup*

Figure 11. Effect of sensor Setup in the number of FP and FN

Results – User-based Evaluation

This section presents the average detection outcomes obtained during the user-based test, using the same response variables considered in the automated evaluation: FP and FN. Table 7 sum- marizes the results across the two parameter combinations and three sensor layouts. Each value represents the average of four repetitions per condition.

Table 7. Average detection outcomes per combination and sensor layout (user-based test). The definitions of Combination A and Combination B are presented in Table 2

Combination	Setup	FP	FN
A	360-degrees	344	4.5
A	End-joint	329	3.75
A	Lateral	0	5.5
B	360-degrees	196	6.25
B	End-joint	168	7.75
B	Lateral	0	9.75

To analyze the effects on detection behavior, an ANOVA was conducted on the FP and FN re- sponse variables, considering the two experimental factors previously described: sensor layout and parameter combination. The assumptions of normality, homoscedasticity, and indepen- dence were verified using the Shapiro-Wilk test, Levene's test, and the Durbin-Watson test, respectively. Table 8 summarizes the obtained p-values.

doi: 10.25100/iyc.v27i2.14759

Table 8. ANOVA assumption verification for the user-based evaluation

Variable	Test	p-value	Significant
FP	Normality	0.0170	TRUE
FP	Homoscedasticity	≤0.001	FALSE
FP	Independence	0.7540	TRUE
FN	Normality	0.3573	TRUE
FN	Homoscedasticity	0.4015	TRUE
FN	Independence	0.7040	TRUE

As observed, the assumptions were met for FN, while FP violated the homoscedasticity assumption. Despite this, the ANOVA can still provide insight, particularly when complemented with graphical exploration. Table 9 displays the significance of the main factors (combination and Setup). Both main factors significantly affected FP, while only the combination factor had a significant effect on FN.

Table 9. ANOVA results for the user-based evaluation

Factor	p-value (FP)	p-value (FN)
Combination	≤0.001	≤0.001
Setup	≤0.001	0.0056

The post-hoc Tukey tests (Table 10) confirmed that, for FP, the Lateral layout resulted in significantly fewer false positives than the other two configurations. As shown in Figure 12a, the median number of FP for the Lateral configuration is zero. This zero median value contributes to the non-homoscedasticity observed in the FP analysis, as indicated in the second row of Ta- ble 8. Furthermore, the post-hoc Tukey tests indicate that there are no significant differences in the number of FP between the End-joint and 360-degrees configurations. Regarding the com- bination factor, the first row of Table 10 indicates that combination B results in a significantly lower number of FP compared to configuration A (A and B were defined in Table 2).

Table 10. Post hoc contrast for the response variable FP (user-based test)

Factor	Contrast	Estimate	p-value
Combination	B - A	−103.00	≤0.001
Setup	End-joint- 360-degrees	−21.50	0.6034
Setup	Lateral- 360-degrees	−270.25	≤0.001
Setup	Lateral- End-joint	−248.75	≤0.001

As no significant differences in FN were associated with the Setup factor (Table 9 and Fig- ure 12b), the post-hoc Tukey test was conducted only for the combination factor (Table 11). This test revealed that, in contrast to the FP results, combination B exhibited an average of approximately 3.33 more FN than combination A.

doi: 10.25100/iyc.v27i2.14759

Table 11. Post hoc contrast for the response variable FN (user-based test)

Factor	Contrast	Estimate	p-value
Combination	B - A	3.33	≤ 0.001

Figure 12a presents the distribution of FP across the three sensor layouts. The Lateral configu- ration consistently yielded zero FP values. This outcome is explained by its sensor placement: due to the reduced number and positioning of sensors in this setup, certain events that could be interpreted as false detections—such as the robot sensing its own body—are not within its detection range. Therefore, the absence of FP in this configuration reflects a physical limitation in detection coverage rather than a performance improvement. In contrast, both the 360-degrees and End-joint configurations reported higher and more variable FP values, likely due to their broader sensing coverage, which increases the chance of detecting unintended objects.

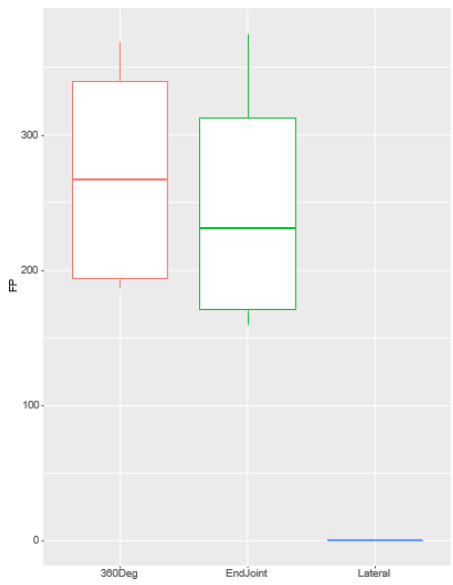

(a) FP as a function of the sensor *Setup* (user-based test)

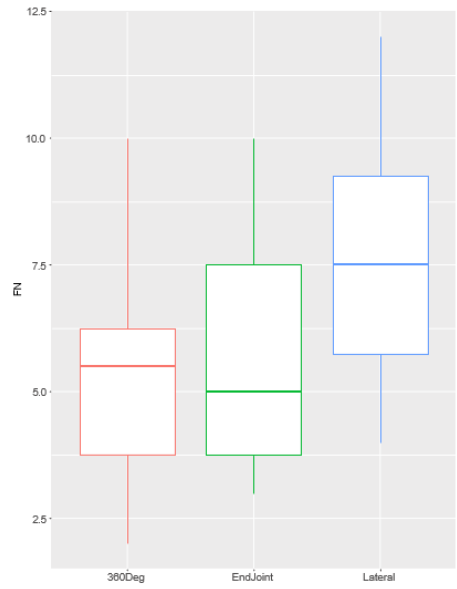

(b) FN as a function of the sensor *Setup* (user-based test)

Figure 12. Effect of sensor Setup in the number of FP and FN (user-based test)

Figure 12b shows the false negatives (FN) distribution. In this case, the Lateral configuration exhibited the highest FN values, followed by 360-degrees and End-joint. This pattern is con- sistent with the detection coverage of each setup: the limited range of the Lateral configuration increases the likelihood of undetected objects or user movement within the shared space, while the EndJoint configuration achieved the lowest FN values, likely due to a more direct and con- sistent view of the interaction area.

doi: 10.25100/iyc.v27i2.14759

Discussion

This study proposed a Unity 3D virtual reality simulator for evaluating sensor configurations in a UR3 collaborative robot. While prior studies do not specify the rationale behind the choice of sensor configurations, particularly regarding their placement on different parts of the robot, common trends in sensor positioning have been observed. These trends have been replicated in the simulator based on the positions of sensors reported in previous research (11, 22, 23, 24, 26, 31, 32, 45, 46, 47, 48, 49, 50). In addition to sensor layouts, this study also considered the factors: Distance, Angle, Sampling, Noise, and Setup.

Interpretation of automated evaluation results

The ANOVA test revealed that among the five factors considered in the experiment, only Dis- tance, Angle, and Setup had a significant effect on the response variables. The Distance and Angle factors exhibited opposite effects on FP and FN, meaning that increasing one of these factors decreases one response variable while increasing the other. This trade-off between FP and FN complicates parameter optimization. For instance, when the maximum detection dis- tance is 15 cm, the number of FP is at its lowest level, whereas FN is maximized. Similarly, when the Angle factor is set to 25°, FP reaches its maximum value while FN is minimized.

Regarding the sensor layouts, the results show contrasting behaviors. The Lateral configuration completely eliminated false positives in both parameter combinations. This outcome, however, is not necessarily indicative of superior performance, but rather a consequence of its reduced sensing coverage. In the Lateral layout, sensors are placed on the sides of the robot, limiting their ability to detect objects directly above or below the end-effector—including the robot's own body. As a result, some real obstacles go undetected, and the system produces fewer FP simply because it fails to detect at all in those directions. This behavior explains the increase in FN observed with this layout, particularly under more constrained parameter settings. Con- versely, the End-joint layout showed the lowest FN values, suggesting better overall detection in critical zones of interaction.

Implication of results

The comparison of sensor layouts revealed that although the Lateral configuration eliminates FP, it does so at the cost of increasing FN due to its limited coverage. In contrast, the End-joint layout offers a more balanced performance, especially in minimizing FN in regions close to the end-effector—critical for safety in collaborative settings. Therefore, to refine the selection of optimal parameters, it becomes necessary to analyze not only the qualitative behavior of each layout, but also the sensitivity of FP and FN to the numerical factors.

A first approach is to consider the estimates in Table 5, where the values are on the order of hundreds, whereas the absolute value of estimates in Table 6 are below ten. This difference suggests that the mean of the FP probability distribution is nearly two orders of magnitude more sensitive to the factors Distance, Angle, and Setup than the mean of FN. However, the consequences of FP are less severe than those of FN. A FP results in an unnecessary robot stop, increasing the time required for an assembly task but without posing a safety risk, whereas an FN implies a potential collision between the operator and the robot.

doi: 10.25100/iyc.v27i2.14759

Given these considerations, the End-joint configuration is selected, as its median FN value is zero (Figure 12). Under the same safety argument, two possible values for the Distance factor remain: 30 cm and 50 cm, as no significant difference was found between them. Regarding the Angle parameter, an angle of 25° provides a wider detection volume, consequently reducing the number of FP.

Interpretation of the user-based evaluation

The second experiment, which involved real users interacting with the virtual environment within a shared workspace, produced results that partially aligned with those of the automated evaluation. For FP, the ANOVA and post-hoc Tukey tests (Table 10) confirmed that Combi- nation B resulted in fewer FP than Combination A, and that the Lateral layout consistently achieved zero FP. In contrast, for FN, the effect of the combination factor was reversed: the average number of FN for Combination A was significantly lower than for Combination B (Ta- ble 11). The statistical analysis further revealed that no significant differences in FN were observed between the different sensor layouts.

However, interpreting the user-based results requires caution. Unlike the controlled automated simulations, human behavior introduces variability and unpredictability. Participants may have unconsciously adjusted their trajectories to minimize close interactions with the robot, which could have reduced the occurrence of FN and masked the consequences of suboptimal sensor configurations. Additionally, while in the automated test each parameter change had a clear and measurable effect, in the user-based evaluation those effects were often attenuated by the user's adaptive behavior.

Therefore, while the user-based test provides preliminary validation for some of the automated findings, it should be considered an approximation rather than a definitive confirmation. For future work, it is recommended to develop standardized and more constrained user protocols that limit behavioral variability and enable more rigorous comparison across conditions.

Nonetheless, the simulator developed in this study represents a significant contribution to the field. It provides a controlled, repeatable, and safe environment for testing sensor layouts before deployment in physical systems. By allowing flexible manipulation of sensor types, positions, and configurations, the simulator enables rapid evaluation of different setups without the cost or risk associated with real-world trials. This makes it a practical tool for optimizing safety configurations in collaborative robotics and supports early-stage design decisions grounded in quantitative evidence.

Limitations

While this study offers valuable insights into the configuration and evaluation of distance sen- sors in collaborative human-robot settings, several limitations must be considered when inter- preting the results.

The experiments were conducted in a virtual reality environment which, although capable of simulating relevant spatial and interactive dynamics, does not replicate all the physical complexities

doi: 10.25100/iyc.v27i2.14759

of real-world industrial settings. Variables such as lighting conditions, tem- perature, occlusions, environmental obstacles, or sensor degradation were not modeled, and these may significantly affect sensor performance in real deployments.

The user-based evaluation, while providing an important perspective on human-robot interaction, should be regarded as exploratory. The unpredictability of human behav- ior—such as voluntary avoidance of collisions—can mask the influence of certain sensor configurations. This variability limits the repeatability and precision of the results, making it difficult to isolate the effects of the tested parameters.

The study focused on a single robot model (UR3) and a limited set of sensor placements. While this offered control over experimental conditions, the findings may not generalize to robots with different kinematics, dimensions, or applications. Broader validation is required to confirm the adaptability of the proposed configurations across various plat- forms.

The analysis was limited to FP and FN as performance indicators. Other relevant met- rics—such as reaction time, task efficiency, or ergonomic impact on the operator—were not addressed and could enrich the evaluation of safety and usability in future studies.

Additionally, practical aspects of sensor integration, such as real-time data processing, system latency, sensor calibration, and economic feasibility, were beyond the scope of this study. These challenges may significantly affect the implementation of sensor-based safety systems in real manufacturing contexts.

Future works

Future research should aim to refine the evaluation of sensor configurations by addressing the variability observed in human-in-the-loop testing. Although the user-based experiment in this study provided valuable insights, the inherent unpredictability of human behavior can obscure the effects of certain parameter changes. Standardized and more constrained user protocols would help minimize this variability and enable more consistent comparisons across configura- tions and users.

In parallel, exploring alternative sensing technologies could enhance the reliability and flexibil- ity of collaborative robotic systems. Vision-based systems, for example, can offer richer contex- tual awareness by identifying and tracking human operators in real time, while millimeter-wave (mmWave) radar sensors provide precise depth perception and are less sensitive to lighting and occlusions. These alternatives, though promising, introduce challenges such as higher compu- tational requirements and integration complexity.

Wearable inertial measurement units (IMUs) also represent a promising direction. By capturing human motion directly, IMUs can support predictive models that anticipate potential collisions, improving response times. Combining these modalities through sensor fusion techniques mayyield more robust and adaptable systems capable of operating in diverse environments.

The simulator developed in this study is well-positioned to support these investigations. Its flex- ibility allows for rapid prototyping of new sensor layouts and testing scenarios in a controlled virtual

doi: 10.25100/iyc.v27i2.14759

space, minimizing risks and resource demands. While the current implementation is based on a UR3 robotic platform, the system architecture is adaptable and could be extended to other collaborative robots and industrial contexts.

By advancing the realism of interaction protocols and expanding the range of technologies under evaluation, future work can consolidate the role of simulation tools as practical assets for designing, optimizing, and validating safety systems in human-robot collaboration.

CRediT authorship contribution statement

Conceptualization - Ideas: Carlos F. Rengifo. Data Curation: Juan J. Piamba. Formal analysis: Carlos F. Rengifo. Investigation: Juan J. Piamba. Methodology: Carlos F. Rengifo. Project Management: Carlos F. Rengifo. Resorces: Juan J. Piamba, Software: Juan J. Piamba. Supervision: Carlos F. Rengifo, Diego E. Guzmán. Validation: Carlos F. Rengifo. Visualization - Preparation: Juan J. Piamba. Writing - original draft - Preparation: Juan J. Piamba. Writing - revision and editing - Preparation: Carlos F. Rengifo, Diego E. Guzmán.

Financing: does not declare. Conflicto of interest: does not declare. Etics aspect: does not declare.

References

(1) Gámez López Manuel de Jesús. Formación profesional y el impacto de la industria 4.0. Revista Tecnológica. 2021;14:51-56. http://www.redicces.org.sv/jspui/bitstream/10972/4419/1/RevistaTecnologica2021_Art11.pdf

(2) Arteaga Félix. La cuarta revolución industrial (4RI): un enfoque de seguridad nacional. Documento de trabajo 12/2018. Real Instituto Elcano, 2018. https://media.realinstitutoelcano.org/wp-content/uploads/2021/10/dt12-2018-arteaga-cuarta-revolucion-industrial-enfoque-seguridad-nacional.pdf

(3) Bragança S, Costa E, Castellucci I, Arezes PM. A brief overview of the use of collab- orative robots in Industry 4.0: Human role and safety. Studies in Systems, Decision and Control. 2019;202:641-650. https://doi.org/10.1007/978-3-030-14730-3_68

(4) Zhang Z, Qian K, Schuller BW, Wollherr D. An Online Robot Collision Detection and Identification Scheme by Supervised Learning and Bayesian Decision Theory. IEEE Transactions on Automation Science and Engineering. 2021;18(3):1144-1156. https://doi.org/10.1109/TASE.2020.2997094

(5) Dobra Z, Dhir KS. Technology jump in the industry: human-robot cooperation in pro- duction. Industrial Robot: the international journal of robotics research and application. 2020; https://doi.org/10.1108/IR-02-2020-0039

(6) Chen JH, Song KT. Collision-Free Motion Planning for Human-Robot Collaborative Safety under Cartesian Constraint. 2018;4348-4354. https://doi.org/10.1109/ICRA.2018.8460185

(7) Hu Y, Wang Y, Hu K, Li W. Adaptive obstacle avoidance in path planning of collaborative robots for dynamic manufacturing. Journal of Intelligent Manufacturing. 2023;34(2):789- 807. https://bd.univalle.edu.co/scholarly-journals/adaptive-obstacle-avoidance-path-planning/docview/2766897519/se-2?accountid=174776

(8) Faroni M, Beschi M, Pedrocchi N. Safety-Aware Time-Optimal Motion Planning With Uncertain Human State Estimation. IEEE Robotics and Automation Letters. 2022;7(4):12219- 12226. https://doi.org/10.1109/LRA.2022.3211493

doi: 10.25100/iyc.v27i2.14759

(9) Lei Y, Su Z, Cheng C. Virtual reality in human-robot interaction: Challenges and bene- fits. Electronic Research Archive. 2023;31(5): https://doi.org/10.3934/era.2023121

(10) Tong Z, Hu H, Wu Z, Xie S, Chen G, Zhang S. An Ultrasonic Proximity Sensing Skin for Robot Safety Control by Using Piezoelectric Micromachined Ultrasonic Transducers (PMUTs). IEEE Sensors Journal. 2022;22(18):17351-17361. https://doi.org/10.1109/JSEN.2021.3068487

(11) Tsuji S, Kohama T. Proximity Skin Sensor Using Time-of-Flight Sensor for Human Col- laborative Robot. IEEE Sensors Journal. 2019;19(14):5859-5864. https://doi.org/10.1109/JSEN.2019.2905848

(12) Hernández OG, Morell V, Ramón JL, García GJ, Jara CA. RGBD Data Analysis for the Evaluation of Trajectory Planning Algorithms in Human Robot Interaction Environments for Rehabilitation. Lecture Notes in Networks and Systems. 2023;589:361-372. https://doi.org/10.1007/978-3-031-21065-5_30

(13) Scimmi LS, Melchiorre M, Troise M, Mauro S, Pastorelli S. A Practical and Effec- tive Layout for a Safe Human-Robot Collaborative Assembly Task. Applied Sciences. 2021;11(4):1763. https://doi.org/10.3390/app11041763

(14) Liu HL, Wang LW. Collision-free human-robot collaboration based on context aware- ness. Robotics and Computer-Integrated Manufacturing. 2021;67:101997. https://doi.org/10.1016/j.rcim.2020.101997

(15) Amin FM, Rezayati M, Venn HW, Karimpour H. A mixed-perception approach for safe human-robot collaboration in industrial automation. Sensors. 2020;20(21):6347. https://doi.org/10.3390/s20216347

(16) Huang Z, Yang B, Liu C. RDCa-Net: Residual dense channel attention symmetric network for infrared and visible image fusion. Infrared Physics and Technology. 2023;130:104589. https://doi.org/10.1016/j.infrared.2023.104589

(17) Park J, Sørensen LC, Mathiesen SF, Schlette C. A Digital Twin-based Workspace Moni- toring System for Safe Human-Robot Collaboration. 2022;24-30. https://doi.org/10.1109/ICCMA56665.2022.10011622

(18) Kianoush S, Savazzi S, Beschi M, Sigg S, Rampa V. A Multisensory Edge-Cloud Plat- form for Opportunistic Radio Sensing in Cobot Environments. IEEE Internet of Things Journal. 2021;8(2):1154-1168. https://doi.org/10.1109/JIOT.2020.3011809

(19) Mukherjee D, Gupta K, Chang LH, Najjaran H. A Survey of Robot Learning Strate- gies for Human-Robot Collaboration in Industrial Settings. Robotics and Computer- Integrated Manufacturing. 2022;73:102231. https://doi.org/10.1016/j.rcim.2021.102231

(20) Lanzoni D, Cattaneo A, Vitali A, Regazzoni D, Rizzi C. Markerless Motion Capture and Virtual Reality for Real-Time Ergonomic Analysis of Operators in Workstations with Collaborative Robots: a preliminary study. 2023;1183-1194. https://doi.org/10.1007/978-3-031-15928-2_103

(21) Choi SH, Park KB, Roh DH, Lee JY, Mohammed M, Ghasemi Y. An integrated mixed reality system for safety-aware human-robot collaboration using deep learning and digital twin generation. Robotics and Computer-Integrated Manufacturing. 2022;73:102258. https://doi.org/10.1016/j.rcim.2021.102258

(22) Fonseca D, Safeea M, Neto P. A Flexible Piezoresistive/Self-Capacitive Hybrid Force and Proximity Sensor to Interface Collaborative Robots. IEEE Transactions on Industrial Informatics. 2023;19(3):2485-2495. https://doi.org/10.1109/TII.2022.3174708

(23) Wu H, Wang X, Li Y. Placement Optimization of Flexible Proximity Sensors for Human- Robot Collaboration. IEEE Robotics and Automation Letters. 2024;9(6):5591-5598. https://doi.org/10.1109/LRA.2024.3396105

(24) Nguyen TD, Kim T, Noh J, Phung H, Kang G, Choi HR. Skin-Type Proximity Sensor by Using the Change of Electromagnetic Field. IEEE Transactions on Industrial Electronics. 2021;68(3):2379-2388. https://doi.org/10.1109/TIE.2020.2975503

(25) Xing C. Perspective of Proximity Sensors on Robots Using Cross-Thought. Highlights in Science, Engineering and Technology. 2023;38:875-887. https://doi.org/10.54097/hset.v38i.5973

(26) Tsuji S, Kohama T. Self-Capacitance Proximity and Tactile Skin Sensor With Shock- Absorbing Structure for a Collaborative Robot. IEEE Sensors Journal. 2020;20(24):15075- 15084. https://doi.org/10.1109/JSEN.2020.3011701

(27) Malik AA, Masood T, Bilberg A. Virtual reality in manufacturing: immersive and col- laborative artificial-reality in design of human-robot workspace. International Journal of Computer Integrated Manufacturing. 2020;33: https://doi.org/10.1080/0951192X.2019.1690685

(28) Aschenbrenner D, Tol DH, Rusák Z, Werker C. Using Virtual Reality for scenario-based Responsible Research and Innovation approach for Human Robot Co-production. Pro- ceedings - 2020 IEEE International Conference on Artificial Intelligence and Virtual Reality (AIVR). 2020;146-150. https://doi.org/10.1109/AIVR50618.2020.00033

(29) Nenna F, Orso V, Zanardi D, Gamberini L. The virtualization of human-robot interac- tions: a user-centric workload assessment. Virtual Reality. 2022;27(9):1-19. https://doi.org/10.1007/s10055-022-00667-x

(30) Havard V, Jeanne B, Lacomblez M, Baudry D. Digital twin and virtual reality: a co- simulation environment for design and assessment of industrial workstations. Production & Manufacturing Research. 2019;7:472-489. https://doi.org/10.1080/21693277.2019.1660283

(31) Xu B, Zhong L, Zhang G, Liang X, Virtue D, Madan R. CushSense: Soft, Stretchable, and Comfortable Tactile-Sensing Skin for Physical Human-Robot Interaction. 2024;5694- 5701. https://doi.org/10.1109/ICRA57147.2024.10610014

(32) Escobedo C, Strong M, West M, Aramburu A, Roncone A. Contact Anticipation for Physical Human-Robot Interaction with Robotic Manipulators using Onboard Proximity Sensors. 2021 IEEE/RSJ International Conference on Intelligent Robots and Systems (IROS). 2021;7255-7262. https://doi.org/10.1109/IROS51168.2021.9636130

(33) Li S, Zheng P, Liu S, Wang Z, Wang XV, Zheng L. Proactive human-robot collaboration: Mutual-cognitive, predictable, and self-organising perspectives. Robotics and Computer- Integrated Manufacturing. 2023;81:1-30. https://doi.org/10.1016/j.rcim.2022.102510

(34) Phan PT, Chao PC, Cai JJ, Wang YJ, Wang SC, Wong K. A novel 6-DOF force/torque sensor for COBOTs and its calibration method. IEEE International Conference on Ap- plied System Innovation (ICASI). 2018;2018:1228-1231. https://doi.org/10.1109/ICASI.2018.8394511

(35) Scimmi LS, Melchiorre M, Mauro S, Pastorelli SP. Implementing a Vision-Based Col- lision Avoidance Algorithm on a UR3 Robot. 2019 23rd International Conference on Mechatronics Technology (ICMT). 2019;1-6. https://doi.org/10.1109/ICMECT.2019.8932143

(36) Melchiorre M, Scimmi LS, Pastorelli SP, Mauro S. Collison Avoidance using Point Cloud Data Fusion from Multiple Depth Sensors: A Practical Approach. 2019 23rd In- ternational Conference on Mechatronics Technology (ICMT). 2019;1-6. https://doi.org/10.1109/ICMECT.2019.8932143

doi: 10.25100/iyc.v27i2.14759

(37) Safeea M, Neto P, Béarée R. On-line collision avoidance for collaborative robot ma- nipulators by adjusting off-line generated paths: An industrial use case. Robotics and Autonomous Systems. 2019;119:278-288. https://doi.org/10.1016/j.robot.2019.07.013

(38) Lu S, Xu Z, Wang B. Human-robot Collision Detection Based on the Improved Camshift Algorithm and Bounding Box. International Journal of Control, Automation and Sys- tems. 2022;20(10):3347-3360. https://doi.org/10.1007/s12555-021-0280-0

(39) Süto˝ S, Forgó Z, Tolvaly-Ros¸ca F. Simulation Based Human-robot Co-working. Procedia Engineering. 2017;181:503-508. https://doi.org/10.1016/j.proeng.2017.02.425

(40) Ko D, Lee S, Park J. A study on manufacturing facility safety system using multimedia tools for cyber physical systems. Multimedia Tools and Applications. 2021;80(26-27):1- 18. https://doi.org/10.1007/s11042-020-09925-z

(41) Shu B, Sziebig G, Pieskä S. Human-robot collaboration: Task sharing through Virtual Reality. IECON 2018 - 44th Annual Conference of the IEEE Industrial Electronics Soci- ety. 2018;6040-6044. https://doi.org/10.1109/IECON.2018.8591102

(42) Perez L, Diez E, Usamentiaga R, Garcia FD. Industrial robot control and operator training using virtual reality interfaces. Computers in Industry. 2019;109:114-120. https://doi.org/10.1016/j.compind.2019.05.001

(43) Franklin CS, Dominguez EG, Fryman JD, Lewandowski ML. Collaborative robotics: New era of human-robot cooperation in the workplace. Journal of Safety Research. 2020;74: https://doi.org/10.1016/j.jsr.2020.06.013

(44) Ding Y, Thomas U. Collision Avoidance with Proximity Servoing for Redundant Serial Robot Manipulators. 2020 IEEE International Conference on Robotics and Automation (ICRA). 2020;10249-10255. https://doi.org/10.1109/ICRA40945.2020.9196759

(45) Rupavatharam S, Fan X, Escobedo C, Lee D, Jackel L, Howard R. AmbiSense: Acoustic Field Based Blindspot-Free Proximity Detection and Bearing Estimation. 2023 IEEE/RSJ International Conference on Intelligent Robots and Systems (IROS). 2023;5974-5981. https://doi.org/10.1109/IROS55552.2023.10341766

(46) Hoffmann A, Poeppel A, Schierl A, Reif W. Environment-aware proximity detection with capacitive sensors for human-robot-interaction. 2016 IEEE/RSJ International Con- ference on Intelligent Robots and Systems (IROS). 2016;145-150. https://doi.org/10.1109/IROS.2016.7759047

(47) Schöffmann C, Ubezio B, Muehlbacher-Karrer S, Zangl H. Radar Sensors in Collaborative Robotics: Fast Simulation and Experimental Validation. 2020 IEEE International Conference on Robotics and Automation (ICRA). 2020;10452-10458. https://doi.org/10.1109/ICRA40945.2020.9197180

(48) Fan X, Simmons-Edler R, Lee D, Jackel L, Howard R, Lee D. AuraSense: Robot Colli- sion Avoidance by Full Surface Proximity Detection. 2021 IEEE/RSJ International Con- ference on Intelligent Robots and Systems (IROS). 2021;1763-1770. https://doi.org/10.1109/IROS51168.2021.9635919

(49) Fan X, Lee D, Chen Y, Prepscius C, Isler V, Jackel L. Acoustic Collision Detection and Localization for Robot Manipulators. 2020 IEEE/RSJ International Conference on Intelligent Robots and Systems (IROS). 2020;9529-9536. https://doi.org/10.1109/IROS45743.2020.9341719

(50) Schmider E, Ziegler M, Danay E, Beyer L, Buhner M. Is it really robust? Reinvesti- gating the robustness of ANOVA against the normal distribution assumption. Method- ology: European Journal of Research Methods for the Behavioral and Social Sciences. 2010;6(4):147-151. https://doi.org/10.1027/1614-2241/a000016

(51) Delacre M, Lakens D, Leys C. Why Psychologists Should by Default Use Welch's t-test Instead of Student's t-test. International Review of Social Psychology. 2017;30:92. https://doi.org/10.5334/irsp.82

doi: 10.25100/iyc.v27i2.14759